AD-A205 996

# Downslope Propagation and Vertical Directionality of Wind Noise

Presented at the
114th Meeting of the
Acoustical Society of America,
16-20 November 1987, Miami, Florida

William M. Carey
Surface Anti-Submarine Warfare Directorate

R. B. Evans
Syntek Engineering & Computer Services

J. Davis
PSI Marine Sciences

George Botseas
Surface Anti-Submarine Warfare Directorate

DTIC
ELECTE
4 APR 1989
S    D
E

# Naval Underwater Systems Center
**Newport, Rhode Island / New London, Connecticut**

## Preface

This report contains the oral presentation "Downslope Propagation and Vertical Directionality of Wind Noise" given at the 114th Meeting of the Acoustical Society of America, 16-20 November 1987, in Miami, Florida.

Reviewed and Approved:
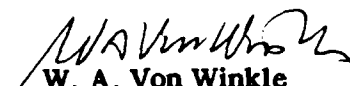
W. A. Von Winkle
Assoicate Technical Director
for Research and Technology

ADA205996

# REPORT DOCUMENTATION PAGE

| 1a. REPORT SECURITY CLASSIFICATION  UNCLASSIFIED | 1b. RESTRICTIVE MARKINGS |
|---|---|
| 2a. SECURITY CLASSIFICATION AUTHORITY | 3 DISTRIBUTION / AVAILABILITY OF REPORT  APPROVED FOR PUBLIC RELEASE  DISTRIBUTION UNLIMITED |
| 2b. DECLASSIFICATION / DOWNGRADING SCHEDULE | |

| 4. PERFORMING ORGANIZATION REPORT NUMBER(S)  NUSC TD 8497 | 5. MONITORING ORGANIZATION REPORT NUMBER(S) |
|---|---|

| 6a. NAME OF PERFORMING ORGANIZATION  NUSC | 6b. OFFICE SYMBOL  (If applicable)  302 | 7a. NAME OF MONITORING ORGANIZATION |
|---|---|---|

| 6c. ADDRESS (City, State, and ZIP Code).  NEW LONDON LABORATORY  NEW LONDON, CT 06340 | 7b. ADDRESS (City, State, and ZIP Code) |
|---|---|

| 8a. NAME OF FUNDING / SPONSORING ORGANIZATION | 8b. OFFICE SYMBOL  (If applicable) | 9. PROCUREMENT INSTRUMENT IDENTIFICATION NUMBER |
|---|---|---|

| 8c. ADDRESS (City, State, and ZIP Code) | 10. SOURCE OF FUNDING NUMBERS | | | |
|---|---|---|---|---|
| | PROGRAM ELEMENT NO. | PROJECT NO. | TASK NO. | WORK UNIT ACCESSION NO. |

11. TITLE (Include Security Classification)

DOWNSLOPE PROPAGATION AND VERTICAL DIRECTIONALITY OF WIND NOISE

12. PERSONAL AUTHOR(S)

W. M. CAREY, R. B. EVANS, J.A. DAVIS, G. BOTSEAS

| 13a. TYPE OF REPORT | 13b. TIME COVERED  FROM _____ TO _____ | 14. DATE OF REPORT (Year, Month, Day)  1989 Feb. 24 | 15. PAGE COUNT |
|---|---|---|---|

16. SUPPLEMENTARY NOTATION

| 17. COSATI CODES | | | 18. SUBJECT TERMS (Continue on reverse if necessary and identify by block number) |
|---|---|---|---|
| FIELD | GROUP | SUB-GROUP | |
| | | | |
| | | | |

19. ABSTRACT (Continue on reverse if necessary and identify by block number)

Measurements of the vertical noise intensity versus angle [W. Carey and R. Wagstaff, J. Acoust. Soc. Am. 80, 1523-1526 (1986)] show the low-frequency distribution (<200 Hz) to be broadly peaked about the horizontal, whereas the higher-frequency ($\sim$ 400Hz) distribution is peaked at the SOFAR angles ($\sim \pm 15°$) near the axis with a minima at the horizontal. This effect has been attributed to the noise from ships over the basin margins [R. Wagstaff, J. Acoust. Soc. Am. 69, 1009-1014(1981)]. However, since spectral variation along the horizontal is smooth and the effect is observed in sparsely shipped areas of the world, wind noise must be included to explain this effect.

| 20. DISTRIBUTION / AVAILABILITY OF ABSTRACT  ☐ UNCLASSIFIED/UNLIMITED  ☐ SAME AS RPT.  ☐ DTIC USERS | 21. ABSTRACT SECURITY CLASSIFICATION |
|---|---|
| 22a. NAME OF RESPONSIBLE INDIVIDUAL | 22b. TELEPHONE (Include Area Code) | 22c. OFFICE SYMBOL |

DD FORM 1473, 84 MAR            83 APR edition may be used until exhausted            SECURITY CLASSIFICATION OF THIS PAGE
All other editions are obsolete.

R. W. Bannister [J. Acoust. Soc. Am. 79, 41–48(1986)] has attributed this effect to high–latitude winds and shallowing sound channel found in Southern Hemisphere waters. W. Carey [J. Acoust. Soc. Am. 79, 49–59 (1986)] attributed the effect to downslope propagation. Calculations between 50 and 400 Hz of the mid–basin vertical directionality made with ASTRAL and PAREQ with a geoacoustic model were both found to show that the bottom behaves as a low–pass filter as the low–frequency energy at higher angles interacts with the bottom and is converted to low–angle energy in the deep sound channel while, at the higher frequencies and higher angle, energy is absorbed. This low–pass effect is consistent with experimental results. Propagation of low–grazing angle energy from the shelf is prominent in the computational results but not apparent in measured data, perhaps due to bathymetric roughness.

S63        J. Acoust. Soc. Am. Suppl. 1, Vol 82, Fall 1987

# DOWNSLOPE PROPAGATION AND VERTICAL DIRECTIONALITY OF WIND NOISE

W. M. Carey and G. Botseas
Naval Underwater Systems Center

R. E. Evans
SYNTEK Engineering & Computer Services

J. A. Davis
PSI Marine Sciences

Measurements of the vertical noise intensity versus angle [W. Carey and R. Wagstaff, J. Acoust. Soc. Am. 80, 1523-1526 (1986)] show the low-frequency distribution (<200 Hz) to be broadly peaked about the horizontal, whereas the higher-frequency ($\sim$ 400Hz) distribution is peaked at the SOFAR angles ($\sim (\pm 15^{\circ})$ near the axis with a minima at the horizontal. This effect has been attributed to the noise from ships over the basin margins [R. Wagstaff, J. Acoust. Soc. Am. 69, 1009-1014(1981)]. However, since spectral variation along the horizontal is smooth and the effect is observed in sparsely shipped areas of the world, wind noise must be included to explain this effect. R. W. Bannister [J. Acoust. Soc. Am. 79, 41-48(1986)] has attributed this effect to high-latitude winds and shallowing sound channel found in Southern Hemisphere waters. W. Carey [J. Acoust. Soc. Am. 79, 49-59 (1986)] attributed the effect to downslope propagation. Calculations between 50 and 400 Hz of the mid-basin vertical directionality made with ASTRAL and PAREQ with a geoacoustic model were both found to show that the bottom behaves as a low-pass filter as the low-frequency energy at higher angles interacts with the bottom and is converted to low-angle energy in the deep sound channel while, at the higher frequencies and higher angle, energy is absorbed. This low-pass effect is consistent with experimental results. Propagation of low-grazing angle energy from the shelf is prominent in the computational results but not apparent in measured data, perhaps due to bathymetric roughness.

S63          J. Acoust. Soc. Am. Suppl. 1, Vol 82, Fall 1987

1

# SUMMARY

- WIND-DRIVEN NOISE AND DOWNSLOPE PROPAGATION EFFECTS ON MID-BASIN VERTICAL NOISE DIRECTIONALITY

  REVIEW VERTICAL NOISE DIRECTIONALITY DATA

  PRESENT A METHOD OF TREATING DISTRIBUTED SOURCES

  COMPUTED VERTICAL DIRECTIONALITY RESULTS AT 50 Hz, 200 Hz, and 400 Hz

  COMPARISON OF PE AND ASTRAL CALCULATIONS

- RESULTS EMPHASIZE THE IMPORTANCE OF THE DOWNSLOPE PROPAGATION AND INDICATE THAT WIND NOISE MAY BE AN IMPORTANT FACTOR

## SUMMARY

This paper examines the role of wind driven noise and down slope propagation on the mid-basin vertically directional noise field.

The characteristic of the vertically directional noise field is first reviewed using the experimental data of Anderson (1972). This frequency dependent characteristic has a broad maximum near the horizontal at low frequencies and a pronounced "horn- like" appearance at the higher frequencies. Previous work (Wagstaff (1981), Carey and Wagstaff (1986)) has indicated that the broad maximum near the horizontal at the lower frequencies was due to slope reflected noise generated by surface ships and/or the wind. Since the vertical directionality data shows a rather smooth frequency characteristic, wind noise was speculated to be important.

This paper presents a technique for computing the noise field at the middle of an oceanographic basin from near surface distributed sources. The computational techniques provides a means for assessment of the down-slope conversion process. Results of calculations of vertical beam noise intensity are presented at frequencies of 50, 200, and 400 Hz. These computational results clearly show that the down slope conversion process acts as a low pass filter determining the vertical noise field at mid-basin. These calculations are based on a noise source level corresponding to a 10 knot wind speed taken from the work of Burgess and Kewley (1983) showing that wind driven noise is indeed an important factor.
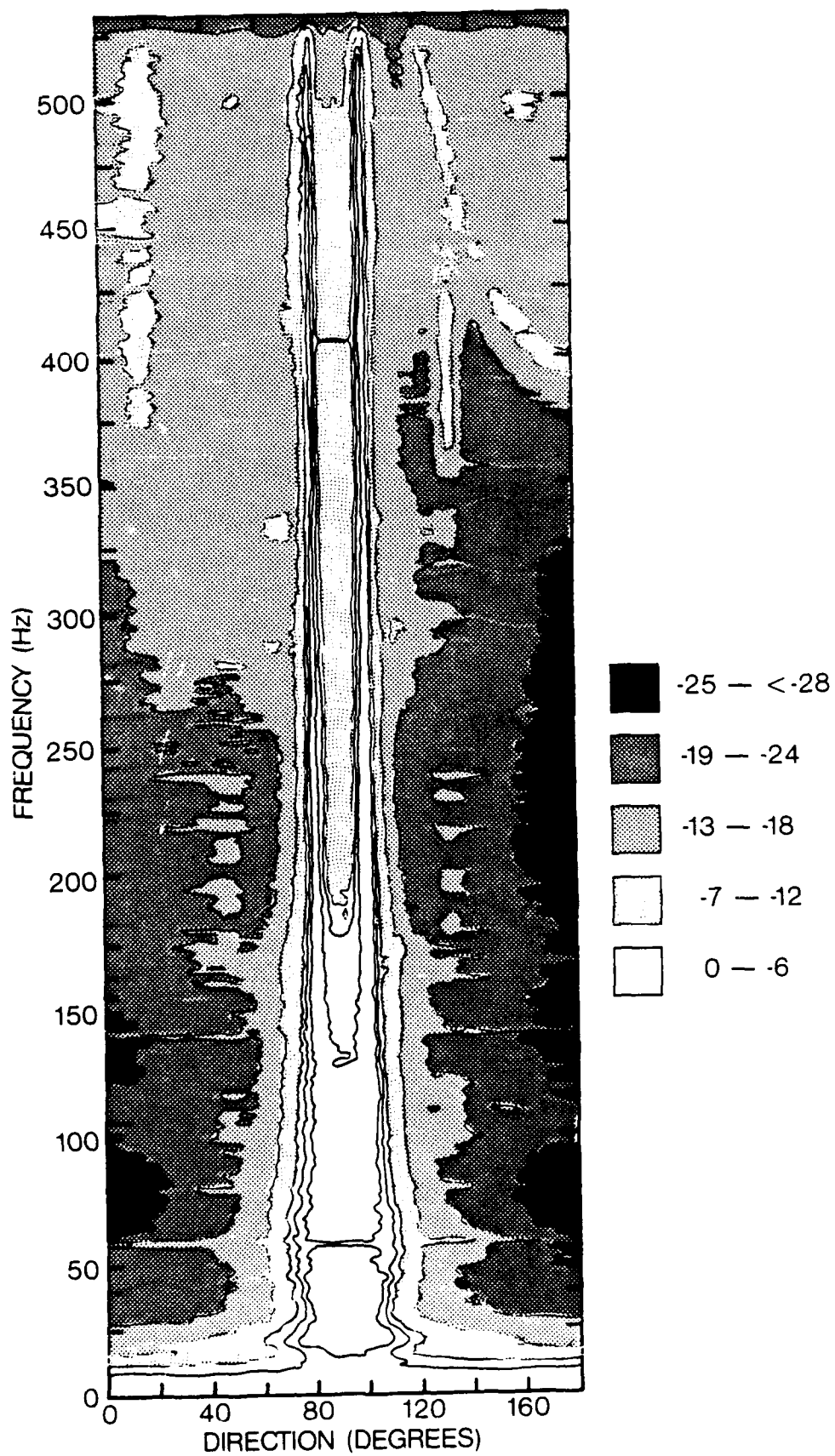
## AMBIENT NOISE VERTICAL DIRECTIONALITY

Since high-angle energy from deep ocean noise sources is rapidly attenuated due to multiple bottom interactions, one would expect the energy propagated from these sources to be peaked at the SOFAR channel ray limiting angles ($10°$ to $15°$ off the horizontal). However, measurements of the vertical distribution of noise intensity in the LF band show a broad angular distribution centered about the horizontal direction. Consequently, the broad distribution of energy about the horizontal requires a mechanism such as the downslope conversion process. These two vugraphs represent a remarkable set of data collected by Anderson (1972) which illustrate these effects. Here, the maximum likelihood method (MLM) [Edelblute (1966)] was used to produce the vertical noise level distribution as a function of vertical angle ($90°$ is the horizontal direction) and frequency. These data were obtained south of Bermuda with a vertical array of 26 elements spanning a distance of 110 m centered at a depth of 236 m in the deep sound channel with an axis depth of 1 km. This vugraph shows the vertical arrival structure of the noise as a function of frequency with resolution of 1.4 Hz. At 150 Hz, the noise intensity has maxima at $90° \pm 9.5°$ compared to $90° \pm 14°$ if the array center had been located at the sound channel axis. The Mimi sound source is observed near 400 Hz. At frequencies greater than 400 Hz, the data show aliasing ($180° - 130°$) and the peaked distribution of noise intensity at $90° \pm 9.5°$ with a noise minima at $90°$ of $- 10$ dB. In comparison, the distribution at 100 Hz shows a broad maximum centered on the horizontal. Anderson was able to simulate the pattern at the higher frequencies but not able to do so at the lower frequencies. He showed that the broad maximum was not due to deficiencies in the measurement technique and analysis. These characteristics persisted for several days; that is, the vertical distribution of energy was broad at the lower frequencies and sharply dual peaked at the higher frequencies, indicating

5
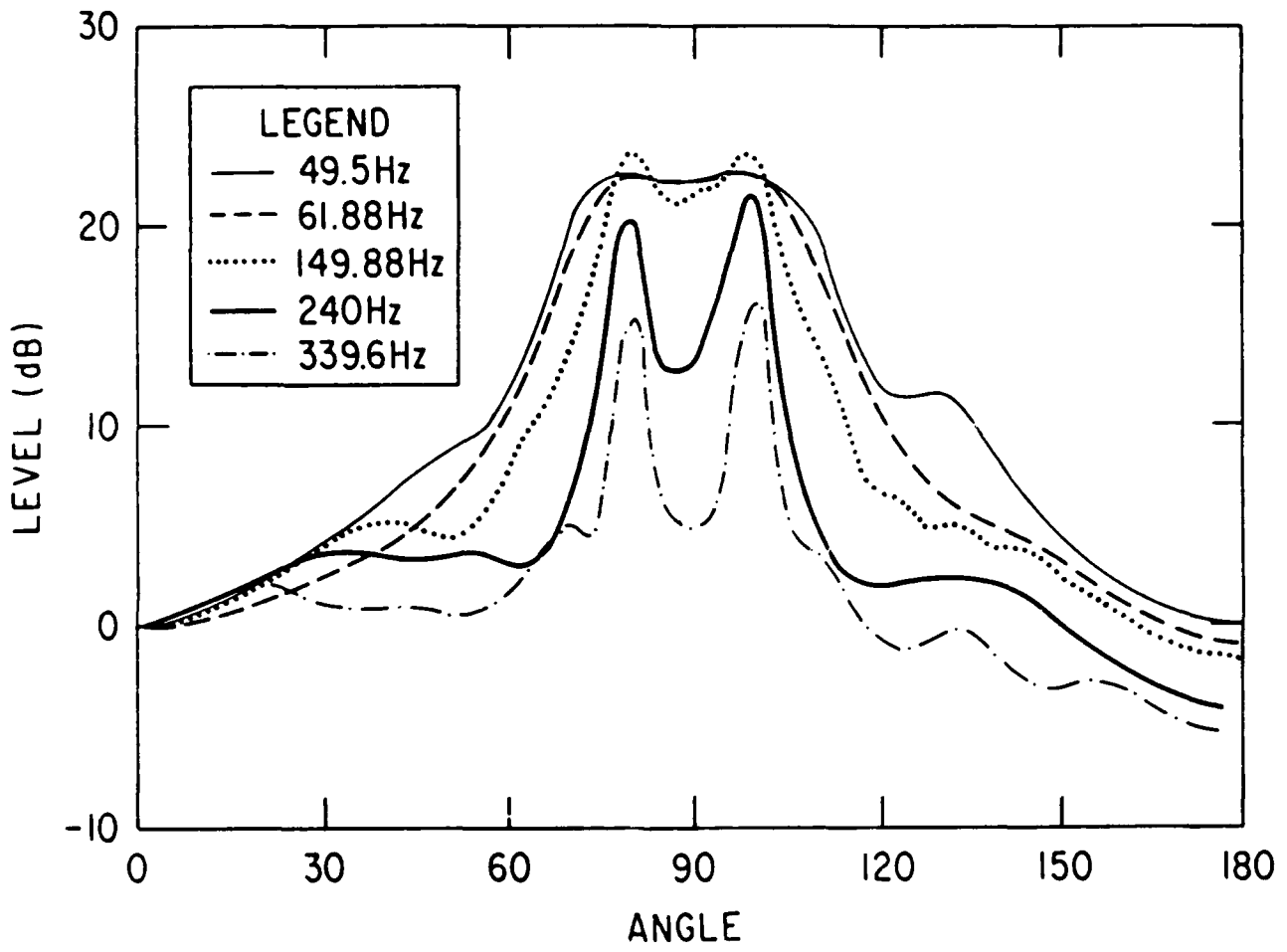
that the horizontal component of noise originates at a distance from the receiver. The smooth noise level variation between 20 and 150 Hz is a significant characteristic of the noise. If the horizontal noise is from distant slope-interacted, ship-radiated signatures, why the smooth frequency variation of the horizontal noise intensity?

These results are consistent with previous and subsequent investigations. Fox (1964) obtained data from a 40-element array near Bermuda in 4.4 km of water. He found that at low sea states, the vertical distribution of noise intensity was broadly peaked near the horizontal over the band of 200 to 1500 Hz. At high sea states, he observed an isotropic distribution at higher frequencies (>200 Hz) but a persistent horizontal component (<200 Hz). Measurements by Axelrod (1965) showed a strong low-frequency horizontal component and observed that the frequency at which the vertical directionality became isotropic depended on the local wind speed. Anderson (1979) reported noise vertical directionality in a region of the Northeast Pacific Ocean over the 23- to 104-HZ band. He also observed a broad angular distribution of noise near the horizontal. A horizontally stratified, range-independent, ocean model does not predict a broad angular distribution of noise intensity about the horizontal, but rather a dual peaked noise intensity distribution ($\pm$ $10^{o}$ to $\pm$ $15^{o}$) and no noise at the horizontal.

Noise generated from surface sources cannot arrive within the limiting angles bracketing this minimum referred to as a horizontal noise notch. Wagstaff (1981) showed by agreement between calculations and data that distant shipping over the continental shelf, slope, or a seamount contribute to the broad vertical distribution of low-frequency noise near the horizontal. Data obtained between Cape Hatteras and Bermuda were analyzed in the 45- to 100-Hz band by Wales (1981). These data were found to have a broad vertical distribution near the horizontal. Their plot of corresponding noise level

7

# FIGI BASIN VERTICAL NOISE DATA BROWNING (1982)



(DAY 148 0255-0256 Z)
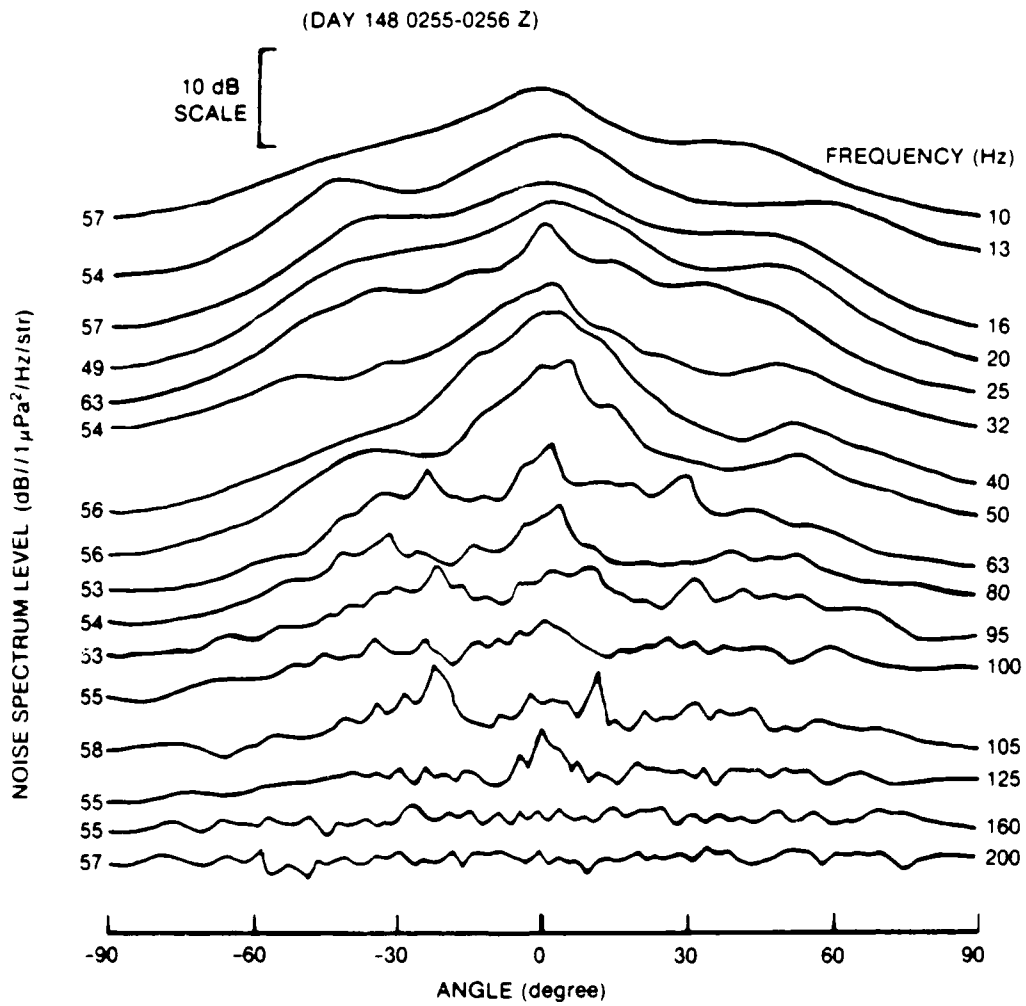
versus frequency and arrival angle shows a smooth variation in frequency similar to that of the Anderson data. The fact that these data do not show a tonal characteristic is important as ship radiated noise spectra have been shown to be primarily tonal in this band. Browning (1982) shows data obtained in the South Figi Basin, a region of sparse shipping as shown in the vugraph. Below 200 Hz, he observed a level 4 dB less than Wagstaff, with broad maximum in the vertical distribution of noise intensity centered at the horizontal. Browning found these results consistent with both surface ship noise and storm noise originating near the basin boundaries coupling to the sound channel. If these results were solely due to radiated sound from ships interacting with slopes and seamounts one might expect the tonal quality of the low-frequency ship signature in the measured noise spectra when the number of ships are small. Since this is not the case, one may draw the inference that another contribution to the noise field at the horizontal is important such as the noise due to wind and surface waves over continental slopes and seamounts. Furthermore, Burgess (1983) has found similar results in Australasian waters.

# Superposition of Noise Sources



$N_j$ = # of sources = $(2\pi\, r_j\, \Delta r)\ \times\ \eta$
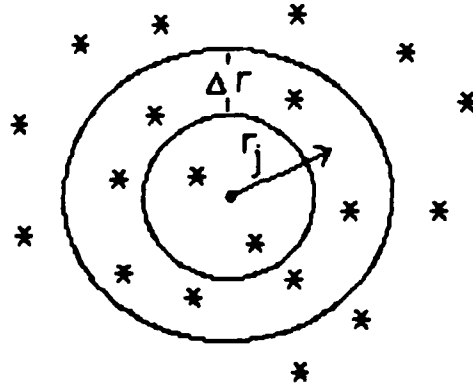
in j th annulus      area   x   density

$$P(r,z) = \sum_{j=1}^{M} e^{i\psi_j} \sum_{k=1}^{N_j} e^{i\phi_k} P(r_j,z)$$

sum on azimuth

sum on range

$$P(r,z) = \sum_{j=1}^{M} e^{i\psi_j} \sqrt{N_j}\ P(r_j,z)$$

$$P(r_j,z) = ( e^{i k_0 r_j} / \sqrt{r_j}\ )\ u(r_j,z)$$

PE field

$$P(r,z) = \sum_{j=1}^{M} e^{i\tilde{\psi}_j} \sqrt{2\pi\, \Delta r\, \eta}\ u(r_j,z)$$

## SUPERPOSITION OF NOISE SOURCES

The radiated pressure at a distance $r_j$ from a single point source at $z_s$ and angle $\theta_{sp}$ to a receiver at $z_m$ is

$$P(z_s, \theta_{sp}, r_j, z_m) = P_o \left[ e^{i k_o r_j} / r_j^{1/2} \right] e^{i\phi_{jp}} \psi(z_m, z_s, \theta_{sp}, r_j),$$

where $\phi_{jp}$ is an arbitrary random phase variable and $\psi$ is the depth dependent "P. E. field". Given an annulus $\Delta r$ about $r_j$ with a density of sources (number/unit area) within the annulus $h$; then the total number of sources at distance $r_j$ is $N_j = 2\pi \Delta r \, r_j \, h$. Summing over the azimuthal angle $\theta_{sp}$ we find:

$$P(z_s, r_j, z_m) = P_o \left[ e^{i k_o r_j} / r_j^{1/2} \right] \psi(z_m, z_s, r_j) \left[ \sum_{p=1}^{N_j} e^{i\phi_{jp}} = \sqrt{N_j} \right].$$

The integrated pressure at the basin center due to J concentric rings of sources is

$$P(z_s, z_m) = \sum_{j=1}^{J} P_o \left[ e^{i k_o r_j} / r_j^{1/2} \right] (2\pi \, r_j \, \Delta r \, h)^{1/2} \psi(z_m, z_s, r_j) e^{i\varphi_j}$$

where $\varphi_j$ is a random variable as each concentric ring of noise sources is independent and random with respect to one another. Simplifying the above equation yields.

$$P_m(z_s, z_m) = (2\pi \Delta r \, h \, P_o^2)^{1/2} \sum_{j=1}^{J} e^{i\phi_j} \psi(z_m, z_s, r_j), \quad \phi_j = k_o \cdot r_j + \varphi_j.$$

We recognize this expression as a superposition of forward marching "PE fields", $\psi(z_m, z_s, r_j)$. The $r_j$ factors have canceled and the term $P_m(z_s, z_m)$ describes the pressure field at an array of N hydrophones.

The output of the array at wave vertical number $k_v$ is

$$b(k_v) = \sum_{m=1}^{N} P_m(z_s, z_m) e^{i\phi_m(k_v)}$$

where $\phi_m(k_v)$ is a phase steering factor.

11

The beam power is then

$$|\beta(k_v)|^2 = b^* b = \sum_{n=1}^{N} \sum_{m=1}^{N} P_n P_m^* \exp(i(\phi_n'(k_v) - \phi_m'(k_v)))$$

$$= \sum_{n=1}^{N} \sum_{m=1}^{N} \sum_{j=1}^{J} \sum_{p=1}^{J} (2\pi \Delta r h P_0^2) \exp(i \Delta \phi_{jp}) \Psi_{nj} \Psi_{mp}^* \exp(i \Delta \phi_{nm}').$$

Since $\phi_j'$, and $\phi_p$ are random independent variables the cross terms in the range summation are equal to zero ( $p \neq j$ ).

$$|\beta(k_v)|^2 = (2\pi \Delta r h P_0^2) \sum_{j=1}^{J} \left[ \sum_{n=1}^{N} \sum_{m=1}^{N} \exp(i \Delta \phi_{nm}') \Psi_n \Psi_m^* \right]$$

$$= (2\pi \Delta r h P_0^2) \sum_{j=1}^{J} |b_j(k_v)|^2.$$

The result of this analysis shows that a PE algorithm can be used to easily calculate the output of a vertical array for any angular sector of a cylindrical basin.  The result further shows that beam forming on the superimposed pressure fields yields the result of a weighted sum of beam intensity inputs at each range step.  The leading term in the above equation also shows that one may specify two factors:  the density of surface distributed sources and the equivalent monopole source strength.

## THE REDUCED WAVE EQUATION

Shown on this vugraph is the reduced wave equation. We have used the convention for the source term $-2 \delta(r)\delta(z-z_s)/r$. The solution to this equation for outward propagating waves is $P(r,z)$. We refer to $k_o = \omega/c_o$ as the carrier, the $\sqrt{r}$ term represents cylindrical spreading and $u(r,z)$ is the range dependent envelope function or PE field. This function satisfies the Parabolic equation. This well known equation clearly shows that the specification of the initial field $g_s(z) = u(0,z)$ allows for the advancing of the solution with range.

# REDUCED WAVE EQUATION

**ELLIPTIC PDE:** $\dfrac{\partial^2 P}{\partial r^2} + \dfrac{1}{r}\dfrac{\partial P}{\partial r} + \dfrac{\partial^2 P}{\partial z^2} + K^2(r,z)P = \dfrac{-2\delta(r)\,\delta(z-z_s)}{r}$

$$K^2(r,z) = K_0^2\, n^2(r,z)\,,\ K_0 = \dfrac{\omega}{C_0}$$

$$P(r,z) = \dfrac{e^{-iK_0 r}}{r^{1/2}}\, u(r,z)$$

**PARABOLIC APPROXIMATION:** $2iK_0\,\dfrac{\partial u}{\partial r} + \dfrac{\partial^2 u}{\partial z^2} + K_0^2\,[n^2(r,z)-1] = 0$

$$u(0,z) = g_s(z)$$

TD 8497

MARCHING ALGORITHM: $u(r + \Delta r, z) = M \lfloor u(r,z) \rfloor$

WITH NOISE: $u(r + \Delta r, z) = M \lfloor u(r,z) + e^{i\psi} g_s(z) \rfloor$
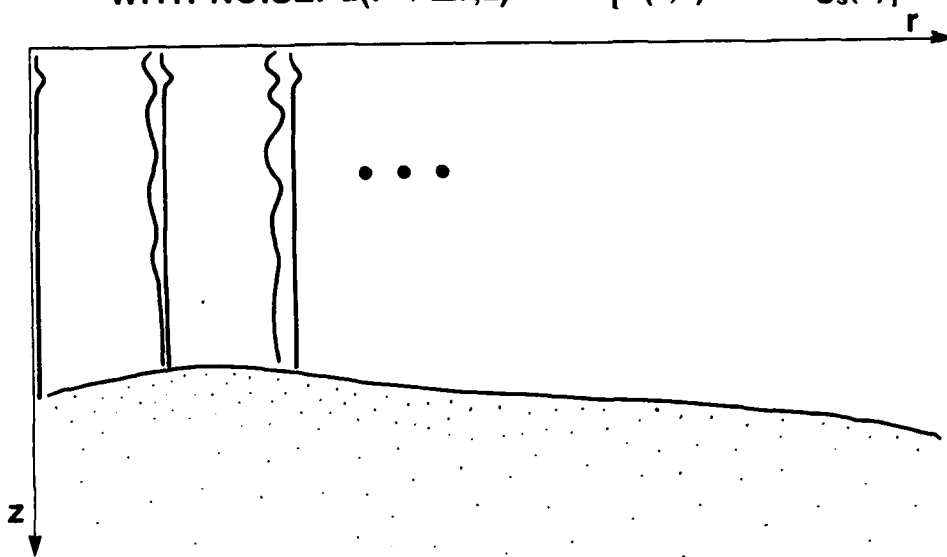
# THE MARCHING ALGORITHM

The advancing of the solution for multiple sources $u(r,z)$ which is a solution to the parabolic equation shown on the previous vugraph is accomplised by the use of a marching algorithm. The field at $r=0$ is determined by a Guassian starting field $g_s(z)$ .

Once the initial field is specified, the field at $r+\Delta r$ is then computed from the field at r by application of the differential operator, or propagator matrix $M$ .

$$u(r+\Delta r, z) = M[u(r,z)]$$

In this calculation the noise is added at each range step. The noise sources are copies of the Gaussian starting field with a random phase $\phi_s$. The Gaussian starting field is chosen for a point source $\lambda/4$ beneath the pressure release surface. The propagator is then applied to obtain the field at $r+\Delta r$ .

$$u(r+\Delta r, z) = M[e^{i\phi_s} g_s(z) + u(r,z)]$$

The resultant field at midbasin due to J rings, a source depth $z_s$ and receiver depth $z_m$ is

$$P(z_m) = \sum_{j=1}^{J} M^{J-1}[e^{i\phi_{sj}} g_s(z_m)] = \sum_{j=1}^{J} exp(i(k_0 r + \varphi_j)) \psi(z_m, z_s, r_j)$$

where

$$M^J = M[M[M[\cdots\cdots]]].$$

We can easily show that addition of the noise source at each range step yields this result.

$$u(z, r_p, z_s) = M(u(z, r_{p-1}, z_s)) + g_s(z, z_s)e^{i\phi_{sp}}$$

It follows by inspection

$$U(z, r_p, z_s) = \sum_{j=1}^{p} M^{J-j} \left[ g_s(z,z_s) e^{i\phi_{s,j}} \right] = \sum_{j=1}^{p} exp(i(k_0 \cdot r_j + \zeta_j)) \psi(z, z_s, r_j)$$

or

$$U(z, r, z_s) = M^{J-1}(g_s e^{i\phi_{s_1}}) + M^{J-2}(g_s e^{i\phi_{s_2}}) \cdots g_s e^{i\phi_{s_J}}$$

thus adding the noise sources at range step with a random phase $\phi_s$ is equivalent to propagation of each noise source to the receiver and summing the resulting pressure fields with a random phase.

# OCEAN BASIN
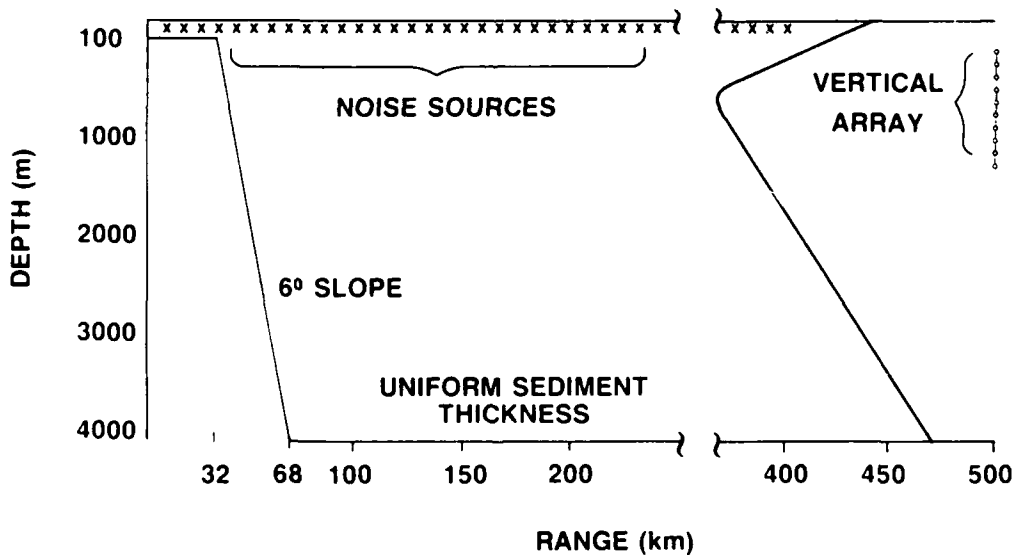
# THE RANGE DEPENDENT OCEAN BASIN

Shown on this vugraph is the stylized ocean basin and sound velocity profile used for these calculations. The slopes are chosen to be $3°$ and $6°$ . The noise sources are uniformly distributed at a depth $z = \lambda/4$ beneath the pressure release surface. The shelf, slope and plain are assumed to be thickly sedimented to avoid computational difficulties associated with rough thinly sedimented boundaries. The depth of the deep basin is taken to be 4000 m. Within 50 km of the vertical array no noise sources are included. We have chosen to eliminate these sources and to concentrate on distant effects. The profile is a representative North Pacific profile. The array was either centered on the sound channel axis or on the critical depth. Samples of the array at various ranges were averaged to obtain the array results.

# BOTTOM MODEL

## SEDIMENT PARAMETERS
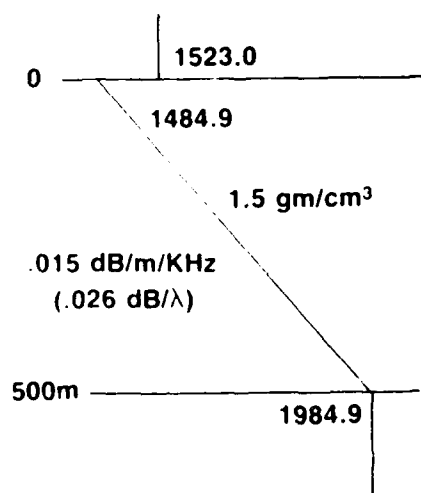
BOTTOM LOSS (dB)
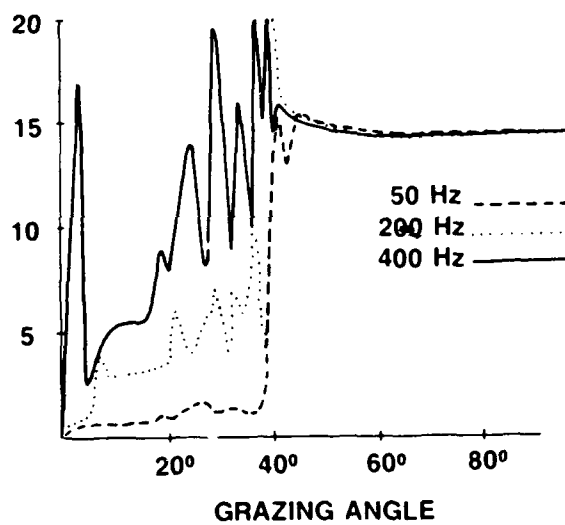
## THE SEDIMENT PARAMETERS AND BOTTOM LOSS

This vugraph shows the geoacoustic model used in the P. E. Code to perform these calculations. The values of the near surface velocity, gradient, attenuation and density are representative of many coastal areas. Also shown is the bottom loss for such a profile at three frequencies, 50, 200, and 400 Hz. The bottom loss curve was determined by the coherent addition of bottom reflected and refracted rays.

## SOURCE LEVEL VERSUS FREQUENCY AND WIND SPEED, KEWLEY (1986)
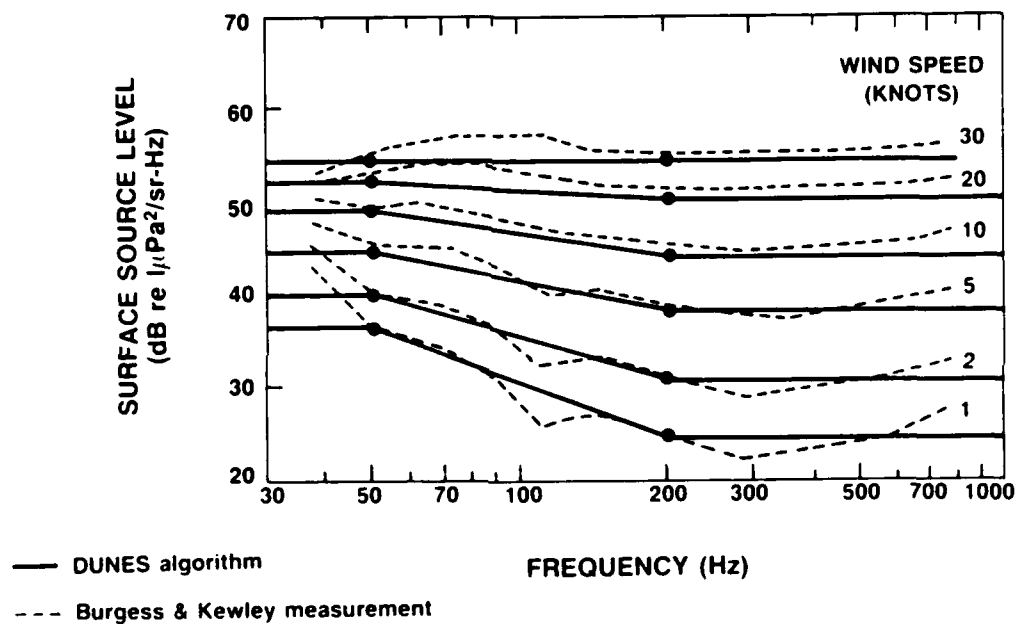
## Wind Generated Ambient Noise Source Levels

For several years we have been examining ambient noise data from omnidirectional hydrophones, horizontal arrays and vertical arrays. Northern hemisphere data for the most part clearly shows the dominance of shipping noise in the low frequency(< 200 Hz) region. However selected Northern Hemisphere data obtained with both omnidirectional hydrophones below critical depth and high resolution vertical arrays, as well as Southern Hemisphere data indicates a wind driven noise mechanism in this low to mid frequency range. The numerical estimation of the properties of mid-basin ambient noise fields which result from wind driven noise requires a determination of the source level and the directional characteristic. Source level estimates which have been published are based on experimental data; however, the conversion from the measured omnidirectional or beam level data needs to be carefully examined. We have encountered difficulty in the direct comparison of published results because of this required conversions to source level. Furthermore the specification of source level in computer codes used to calculate these noise fields also requires care due to the multitude of conventions and the characteristics of the particular propagation model being used. In our opinion, a standard definition of source level and characteristics would have been most helpful. The purpose of this paper is to supply a sound rational and standard specification for wind driven noise source level.

**COMBINED**

MAX. = 49 dB
OMNI = 65 dB
SL = 150 dB

**DEEP BASIN**

MAX. = 47 dB
OMNI = 62 dB
SL = 150 dB

MAX. = 48 dB
OMNI = 61 dB
SL = 150 dB
f = 50 Hz
N = 90 Hydrophones

**SLOPE REFLECTED**

VERTICAL ANGLE   (DEG)
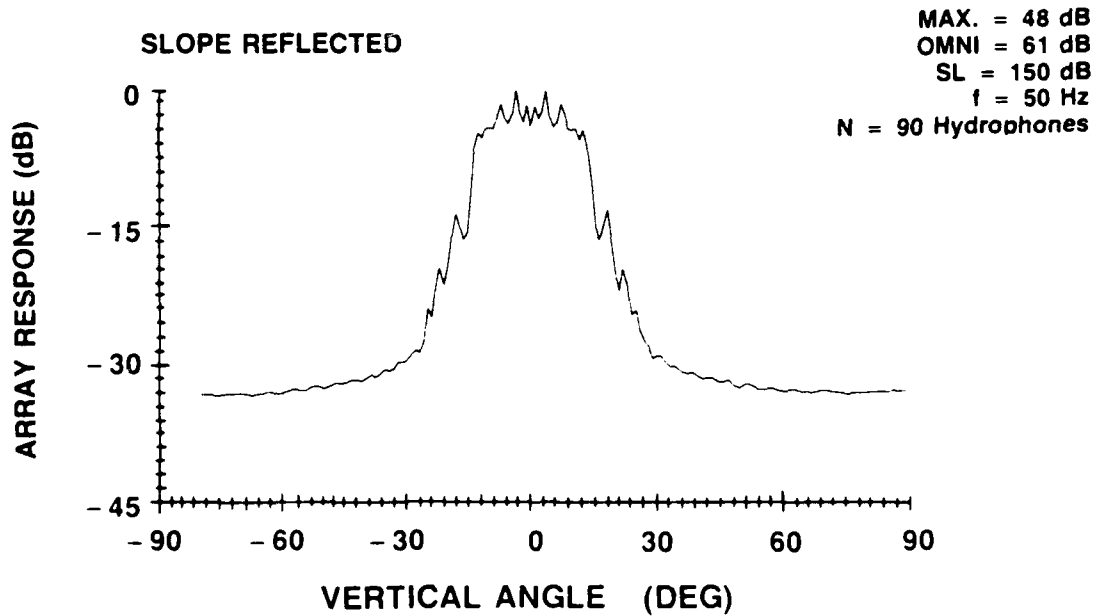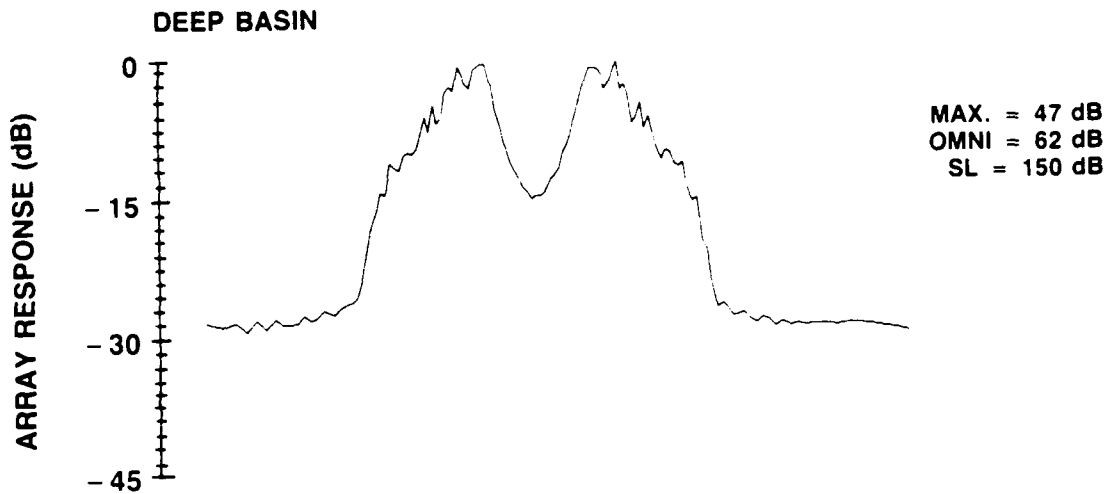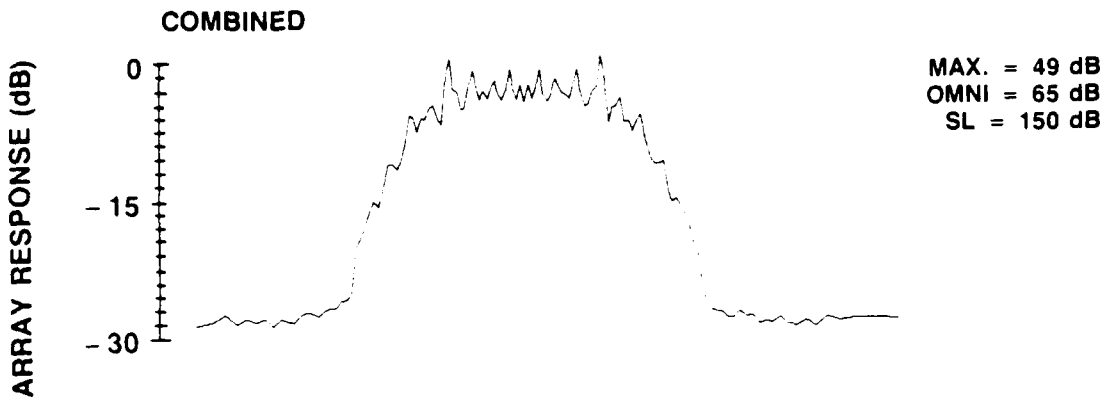
# THE MID-BASIN NOISEFIELD IS COMPOSED OF DEEPWATER AND SLOPE REFLECTED NOISE

## THE MID-BASIN NOISE FIELD DEEP WATER AND SLOPE REFLECTED NOISE

The vugraph shows the result at 50 Hz for a 90 element array equally spaced at $\lambda/2$ centered on the sound channel axis and located at mid-basin. The result represents the average of fifty samples obtained at 1 km range intervals and are for a slope of $6^\circ$. The source level was taken as 50 dB re $/\mu$ Pa consistent with the 10 knot wind speed curve of Burgess and Kewley. At the top of the vugraph we see the broad maximum near the horizontal observed in experimental data. The Deep Basin curve shows a notch at angles near the horizontal as one would expect for a stratified ocean with no boundaries. The slope reflected curve clearly shows a maximum centered along the horizontal confirming the concept that slope reflected wind and shipping noise are responsible for this effect. Also shown on this vugraph are the normalized values of the maximum beam noise level and the omnidirectional noise levels corresponding to a wind source level of 50 dB re $/\mu$ Pa (shown as 150).

ARRAY RESPONSE (dB)

MAX. = 49 dB
OMNI = 65 dB
SL = 150 dB
f = 50 Hz
N = 90 Hydrophones
ΔR = 25 m
DI = 19.5 dB

MAX. = 41 dB
OMNI = 53 dB
SL = 145 dB
f = 200 Hz
ΔR = 625 m
N = 100 Hydrophones
DI = 20 dB

MAX. = 34 dB
OMNI = 45 dB
SL = 142 dB
f = 400 Hz
N = 256 Hydrophones
DI = 24 dB

ANGLE (DEG)
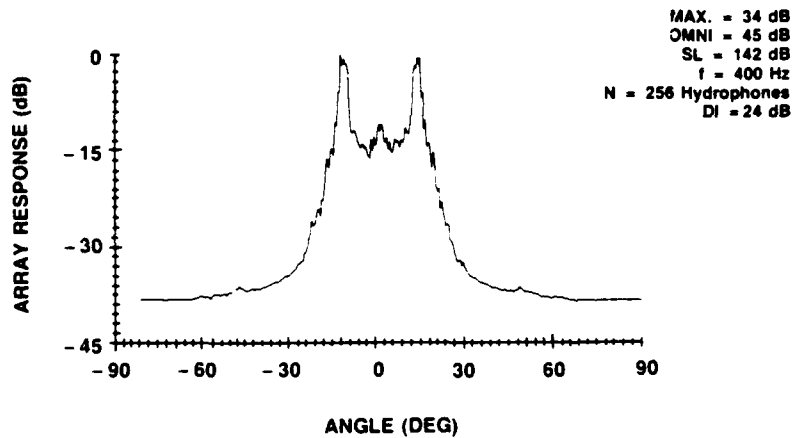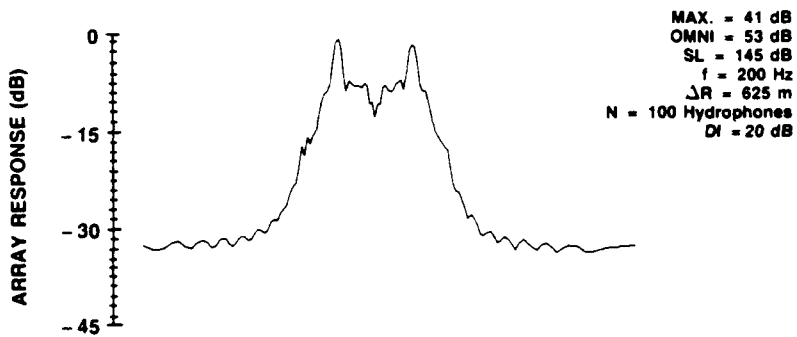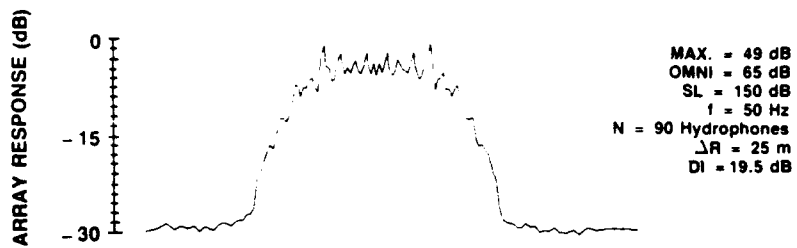
**SLOPE REFLECTED PLUS DEEPWATER NOISE**

## THE MID-BASIN NOISE FIELD AT 50, 200, AND 400 Hz

Shown on this vugraph are the results for 50, 200, and 400 Hz. These results show the development of a noise notch along the horizontal due to the frequency dependent slope reflections. The results are similar to the data presented at the begining of the paper. The 400 Hz results show the notch, some energy along the horizontal and the "horn-like" feature observed in experimental data. These "horn-like" features contain natural wind driven noise as well as distant shipping noise (not considered here). This structure in a real ocean basin should be anisotropic. The wind noise reflecting the variation of the basin boundaries with azimuth and the shipping noise the distribution of ships. The feature near the horizontal at 400 Hz is due to low grazing angle energy from the slope. The feature should change with slope angle and eliminated by real surface roughness.
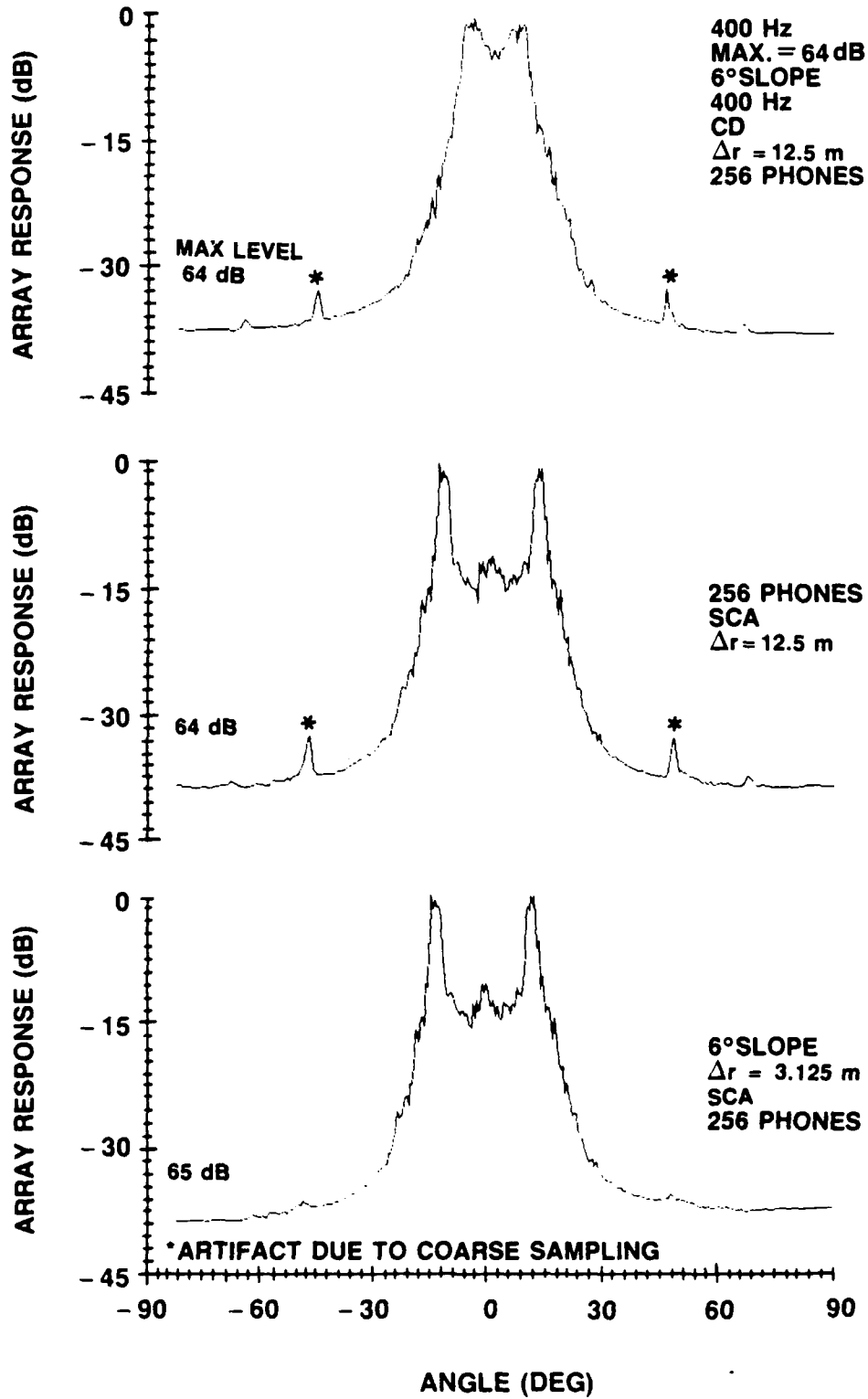
**A COMPARISON OF AN ARRAY WITH 256 ELEMENTS AT CD
AND AT THE SOUND CHANNEL AXIS**

## A COMPARISON OF AN ARRAY WITH 256 ELEMENTS AT CRITICAL DEPTH AND AT THE SOUND CHANNEL AXIS.

The 400 Hz results for an array at the critical depth and at the sound channel axis clearly identifies the change in the shape of the vertical directionality with depth. The bottom curve shows the computational result at the correct range step for the parabolic equation calculation. The top two curves were calculated using a coarse sampling of 12.5 m. Although the results were found to agree, an aliasing artifact was also observed. These results show what the vertical array at critical depth would observe distant source near the horizontal.
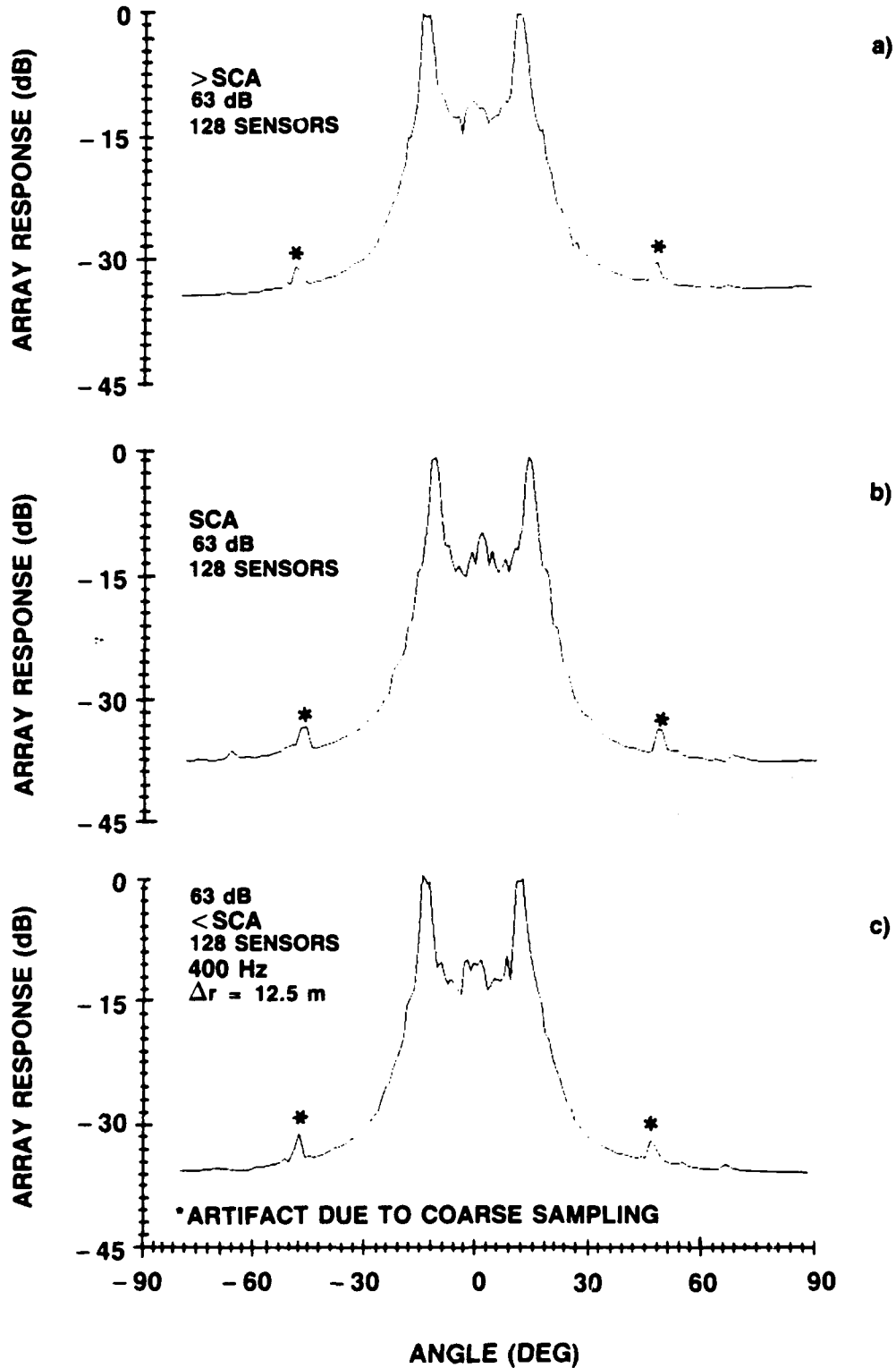
A COMPARISON OF A 128 ELEMENT ARRAY a) ABOVE SCA, b) AT THE SCA, AND c) BELOW THE SCA

## A COMPARISON OF AN ARRAY WITH 128 ELEMENTS

## a) above SCA, b) at the SCA, and c) below the SCA.

This comparison, shown on this vugraph, between an array above the sound channel axis (a), centered on the sound channel axis (b) and below the sound channel axis (c) show that for the deep water sound speed profile employed in these computations a robust feature, "horn-like" structure near ($\pm 12^{\circ}$) and a noise noted centered on the horizontal. The "horn-like" structure is due to the RR/RSR propagation which results from near surface sources. The slope reflectively causes the notch. The central feature along the horizontal is due to low grazing angle energy propagating down the slope and would change with a change in slope or the introduction bottom roughness.
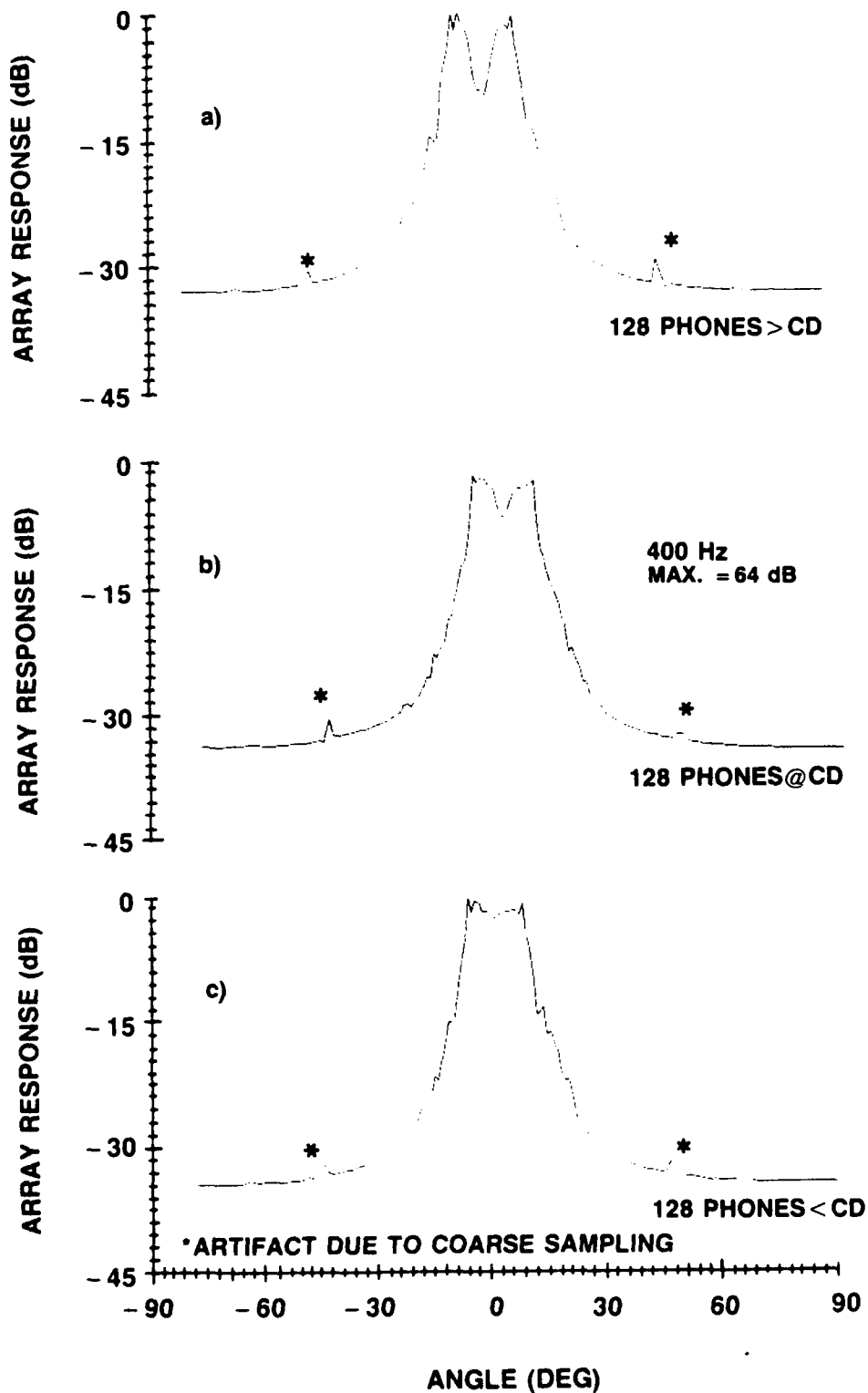
A COMPARISON OF AN 128 ELEMENT ARRAY a) ABOVE C.D.,
b) AT C.D., c) BELOW C.D. SHOWING THE CHANGE IN
VERTICAL STRUCTURE AS DEPTH IS INCREASED

# A COMPARISON OF A 128 ELEMENT ARRAY

## a) Above C. D., b) ATC. D., c) Below C. D.

This vugraph shows the variation of beam noise intensity versus vertical angle near the critical depth (C. D.). Part C shows the remaining elements below critical depth. The noise intensity is centered on the horizontal ($\pm 9^{\circ}$). The 128 element array centered on the C. D., shows a diminution of intensity near the horizontal and the array above critical depth shows a deepening notch. The result is what one would expect from ray tracing; that is, near the sound channel axis, RR and RSR propagation result in propagation near the SOFAR angles and at critical depth near the horizontal due to the turning of rays.

400 Hz
MAX. = 64 dB
CENTERED ON AXIS
6º SLOPE
256 PHONES
$\Delta r$ = 12.5 m
50 SAMPLES

CENTERED ON AXIS
3º SLOPE
256 PHONES
$\Delta r$ = 12.5 m
50 SAMPLES
400 Hz
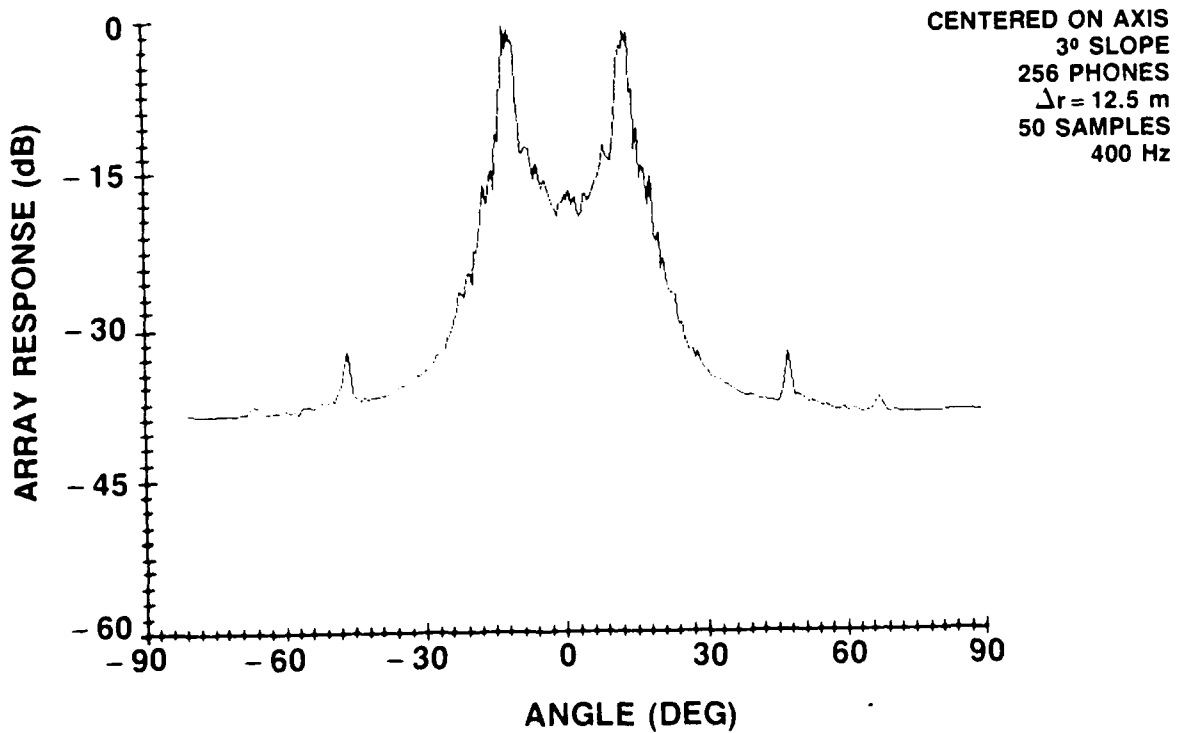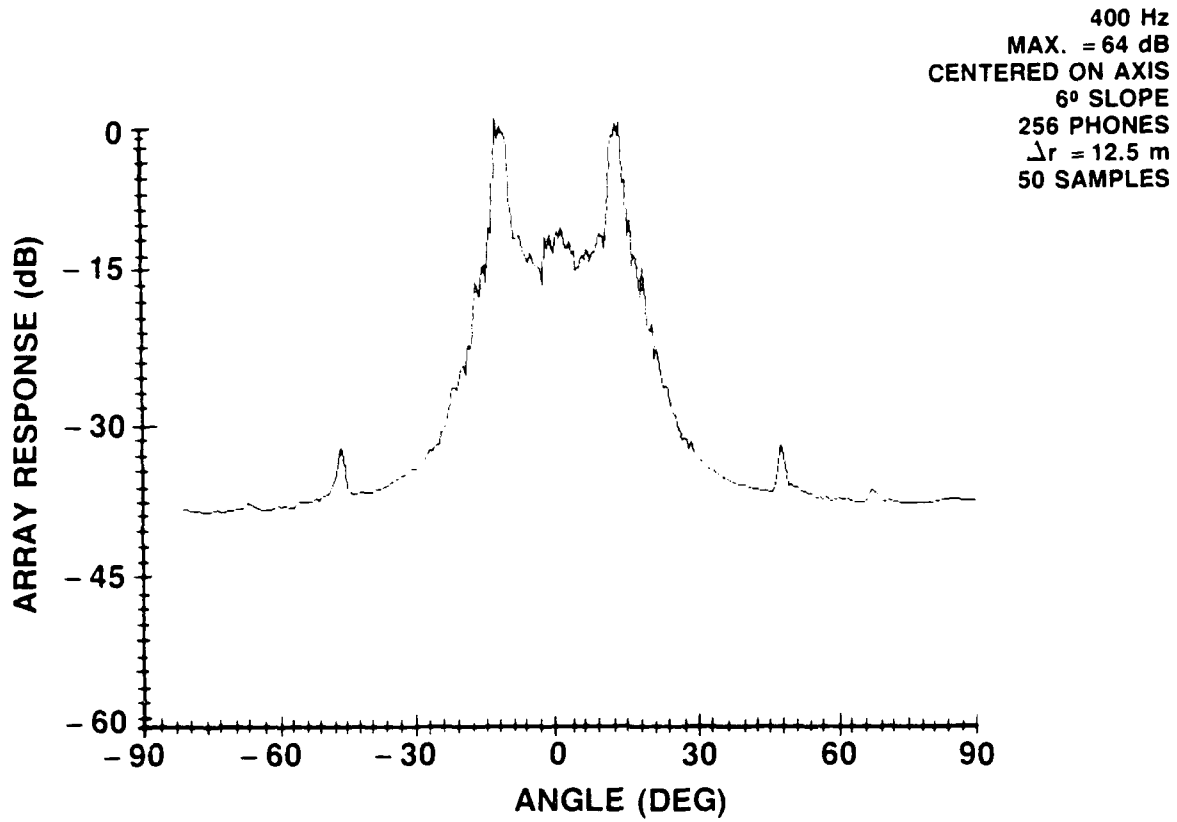
**A COMPARISON OF 6° VERSUS 3° CONTINENTAL SLOPE**

## A COMPARISON OF A 3° THROUGH 6° CONTINENTAL SLOPE

Tnis vugraph shows the result for a 3° through 6° slope. The major effect of changing the slope angle is to reduce the low grazing angle feature observed along the horizontal direction. The basic qualitative structure, the "horn-like" structure, remains as this effect is a consequence of the sound channel. One would expect this structure to change with the properties of the sound channel. Similar channels with a well defined axis will show this qualitative feature with different SOFAR angles. Sound channels which are strictly upward refracting (ARCTIC) and downward refracting (equatorial shallow waters) would have a different characteristic.
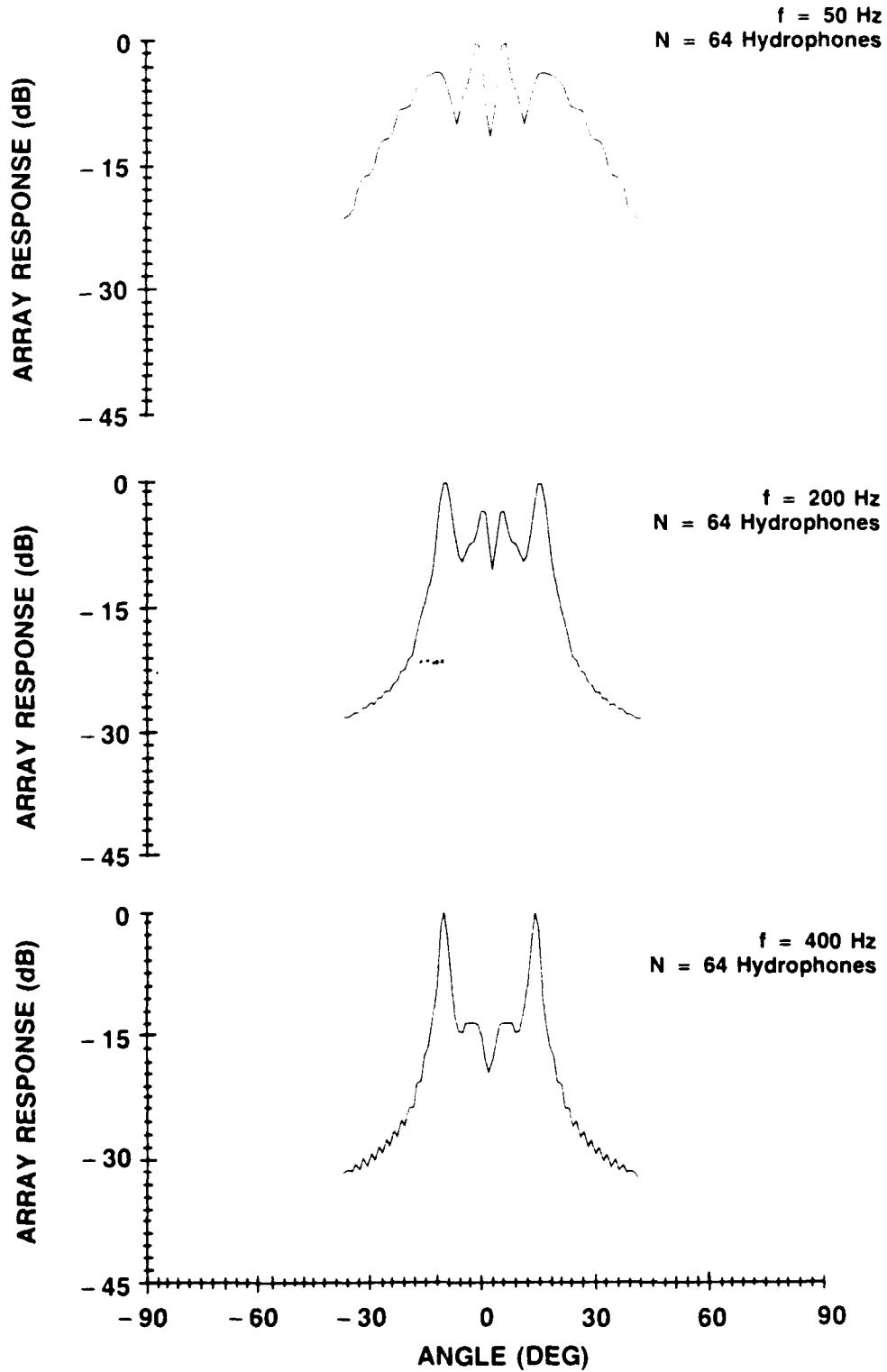
**ASTRAL COMPUTATIONS OF THE VERTICAL FIELD**

## COMPUTATIONS PERFORMED WITH ASTRAL

A modified version of the ASTRAL code was also used to compute the vertical beam noise for essentially the same idealized basin configuration used in the PE calculation. As in the PE case, the wind noise source was represented by a point source a quarter wavelength below the sea surface. Important differences between the two calculations include:

(1) ASTRAL generates range averaged TL and is based on the adiabatic approximation.

(2) ASTRAL, unlike PE, can not distinguish up from down.

(3) A bottom loss vs grazing angle equivalent of the geoacoustical bottom is used in ASTRAL.

(4) Beam noise is computed by intensity convolution of the ASTRAL smode intensity with the appropriate beam pattern.

The resulting beam noise for three 64-element arrays located at the sound channel axis is shown on this vugraph at 50 Hz, 200 Hz, and 400 Hz. In each case the array element spacing is a half-wavelength. The important features to notice are:

(1) the decrease in the beam noise for angles greater than approximately 15 degrees as the frequency increases - - due to the bottom stripping.

(2) the reduction of the SOFAR energy coming from noise sources over the slope and shelf as the frequency increases - - due to higher bottom loss and volume attenuation.

These are the same qualitative features found in the PE calculation. However, the near horizontal beam noise coming from sources over the slope and shelf is dominated by two "spikes" near horizontal contrasted with the smooth behavior of the PE beam noise. We would anticipate that in a real asymmetric

basin with varying slopes, shelf and bottom characteristics these spikes would occur at different angles with varying intensity and the net result would be smoother behavior. We also note that the omni levels compare favorably with PE. Finally, to put these results in perspective we should point out that the ASTRAL calculation required some 2 or 3 minutes CPU time on a Leading Edge PC (regardless of frequency), whereas the PE calculation required approximately 8 hours at 50 Hz and 4 days at 400 Hz on a MICRO-VAX.

# SUMMARY

1. SLOPE REFLECTED NOISE DETERMINES THE HORIZONTAL COMPONENT OF THE MID-BASIN NOISE FIELD

2. THE BOTTOM OF THE SLOPE ACTS AS LOW PASS FILTER

3. CALCULATIONS PERFORMED WITH THE BURGESS/KEWLEY SOURCE LEVEL CURVES AT 10 KNOTS WIND SPEED YIELD:

| FREQ. | OMNI/WENZ | BNL/WENZ |
|-------|-----------|----------|
| 50 | 65/70-80 | 45/50-60 |
| 200 | 54/55-70 | 33/35-50 |
| 400 | 45/44-49 | 18-24/35-40 |

4. COMPARISONS WITH ASTRAL SHOWED QUALITATIVE AGREEMENT BUT DIFFERENCES OF 2db OMNI LEVELS AND 3db WRT BEAM NOISE LEVELS

## SUMMARY

In basins with boundaries, slope and seamount reflected noise contributes to the horizontal intensity component of vertical noise at mid-basin.  In addition to frequency dependent absorption, bottom loss upon reflection from the slope cause the horizontally directed component of the vertical noise field to diminish with frequency, resulting in a notch along the horizontal at the higher frequencies.

These calculations were performed with Burgess-Kewley source levels for a 10 knot wind speed and were calculated to produce mid-basin omnidirectional levels of 68 dB @ 50 Hz, 56 dB @ 200 Hz, and 46 db @ 400 Hz.  The magnitude of these levels indicate that coastal winds can compete with coastal shipping to explain the horizontal component.  These vertical noise intensity levels along the horizontal are consistent with measured levels.

We have compared these computations to those performed with the ASTRAL code. This code is extremely fast and is used in a variety of noise prediction codes.  While differences were found in the vertical noise intensity distribution, a comparison of levels showed that omni levels were within 2dB and beam noise levels 3 dB of the P. E. results.

These results clearly show that the down slope conversion acts as a low pass filter determining the vertical noise field at mid-basin.  These results show that for a 50 dB re $/\mu$ Pa (10 knot wind noise source level) that wind noise could be an important contributor.

# CONCLUSIONS

- WIND DRIVEN NOISE REFLECTED FROM THE OCEAN BOUNDARIES CAN CONTRIBUTE TO THE HORIZONTALLY DIRECTED NOISE AT THE LOWER FREQUENCIES

- DISTRIBUTED NOISE SOURCE CALCULATIONS CAN BE PERFORMED WITH THE BOTSEAS-EVANS TECHNIQUE AND ENABLE THE EVALUATION OF THE RELATIVE IMPORTANCE OF THE VARIOUS MECHANISMS

- CARE MUST BE EXERCISED WHEN ATTEMPTING TO PREDICT THE OUTPUT OF A VERTICAL ARRAY USING ASTRAL

- THIS TECHNIQUE CAN BE USED TO EVALUATE THE EFFECT OF WIND DRIVEN NOISE AND THE SSC ON THE NOISE FIELD OF THE BASINS OF THE SOUTHERN HEMISPHERE

# CONCLUSIONS

Wind driven noise reflected from the ocean boundaries and sea mounts can contribute to the horizontally directed noise at the lower frequencies. In our case the slope acts as a low pass filter determined by the bottom reflectivety. Wind driven noise over the basin determines the minimum level to be achieved in the noise horns.

Distributed noise calculations can be performed with this technique. We have stressed wind driven noise over slopes, however, this computational technique can be used to compute seamount reflected noise and the effect of a shallowing sound channel and the role of high latitude winds.

BIBLIOGRAPHY

Anderson, D. G., D. A. Anderson, D. J. Eldeblute et al., "VLAM Data Analysis Site #1, Bermuda," Naval Ocean Systems Center, TN 800, San Diego, CA, 1972.

Anderson, V. C., "Variation of the Vertical Directionality of Noise with Depth in the North Pacific," Journal of the Acoustical Society of America, vol. 66, 1979, pp. 1445-1452.

Axelrod, E. H., B. A. Schoomer, and W. A. Von Winkle, "Vertical Direction-ality of Ambient Noise in the Deep Ocean at a Site Near Bermuda," Journal of the Acoustical Society of America, vol. 37, 1965, pp. 77-83.

Bannister, R. W., "Deep Sound Channel Noise from High-Latitude Winds," Journal of the Acoustical Society of America, vol. 79. 1986, pp. 41-48.

Browning, D. G., N. Yen, R. W. Bannister, R. N. Denham, and K. M. Guthrie, Vertical Directionality of Low Frequency Ambient Noise in the South Fiji Basin, NUSC Technical Document 6611, Naval Underwater Systems Center, New London, CT, 21 January 1982.

Burgess, A. S., and D. J. Kewley, "Wind-Generated Surface Noise Levels in Deep Water East of Australia," Journal of the Acoustical Society of America, vol. 73, no. 1, 1983, pp. 201-210.

Carey, W. M., and R. A. Wagstaff, "Low-Frequency Noise Fields," Journal of the Acoustical Society of America, vol. 80, no. 5, 1986, pp. 1523-1526.

Eldeblute, D. J., J. M. Fisk, and G. L. Kinnison, "Criteria for Optimum-Signal-Detection Theory for Arrays," Journal of the Acoustical Society of America, vol. 41, 1966, pp. 199-205.

Fox, G. R., "Ambient Noise Directivity Measurements," Journal of the Acoustical Society of America, vol. 36, 1964, pp. 1537-1540.

Wagstaff, R. A., "Low-Frequency Ambient Noise in the Deep Sound Channel -- The Missing Component," Journal of the Acoustical Society of America, vol. 69, 1981, pp. 1009-1014.

Wales, S. C., and O. I. Diachok, "Ambient Noise Vertical Directionality in the Northwest Atlantic," Journal of the Acoustical Society of America, vol. 70, 1981, pp. 577-582.

# INITIAL DISTRIBUTION LIST

| Addressee | No. of Copies |
|---|---|
| CNA | 3 |
| DTIC | 2 |
| DTIC/NAVAL TECHNOLOGY OFFICE (R. Clark, C. Stuart, K. Hawker) | 3 |
| DARPA | 5 |
| CNO (OP-091, -952, NOP-096) | 3 |
| CNR (OCNR-00, -10, -11, -1125 (Marshall Orr, R. Robracta), -13 (K. W. Lackie, K. Dial, E. Chaika), -20, ONT-23, -234, -230) | 12 |
| ONR DET BAY ST. LOUIS | 2 |
| NAVAIRSYSCOM (NAIR-93, -933) | 2 |
| SPACE & NAV WARFARE SYS CMD (PMW-180 (R. Doolittle, J. Synsky, CAPT K. Evans, CAPT R. Witter)) | 4 |
| NAVSEASYSCOM (SEA-63) | 1 |
| NRL (NRL 5100, 5120, 5160, 5130 (N. Yen)) | 5 |
| NORDA (245 (R. Wagstaff), 110 (W. Moseley), 200 (E. Franchie), 240 (R. Farwell), 125L (Library)) | 5 |
| NEPRF | 1 |
| NADC | 1 |
| NCSC | 1 |
| NOSC | 1 |
| DTRC CADEROCK LAB | 2 |
| NSWC WHITE OAK LAB | 2 |
| NPS (Dr. H. Medwin) | 5 |
| NUSC DET AUTEC | 1 |
| NUSC DET WEST PALM BEACH (R. Kennedy) | 1 |
| APL/JOHNS HOPKINS (G. Smith) | 1 |
| APL/U. WASHINGTON (R. Spindel) | 2 |
| ARL/PENN STATE (S. McDanniels, D. McGammon) | 3 |
| ARL/U. TEXAS (S. Mitchell) | 3 |
| MPL/SCRIPPS (F. Fisher, W. Hodgkiss) | 3 |
| WOODS HOLE OCEAN. INSTI. (S. Williams, G. Frisk, J. Lynch) | 5 |
| U. OF MIAMI (F. Tappert, H. DeFarrari) | 2 |
| BOLT BERANEK & NEWMAN, INC. (P. Cable, S. Marshall, W. Marshall, G. Duckworth, P. Smith) | 5 |
| SAI CORP., McLean, VA (A. Eller) | 3 |
| SAI CORP., New London, CT (F. DiNapoli) | 3 |
| SYNTEC (R. Evans) | 1 |
| TRW (S. Gerben) | 1 |
| MIT (H. Schmidt, A. Baggeroer, I. Dryer) | 3 |
| U. OF DELAWARE (V. Klemas, P. Lyrenga, D. Wood) | 3 |
| SEA GRANT OFFICE, AVERY POINT (E. Monahan) | 1 |
| LaJOLLA INSTITUTE | 1 |
| DEFENCE SCIENTIFIC ESTABLISHMENT (Dr. Richard Bannister) | 1 |
| DEFENCE RES. EST. PACIFIC (Dr. Robert Chapman, Dr. R. Chapman) | 2 |
| DEFENCE RES. EST. ATLANTIC (Dr. Harold Merklinger) | 1 |
| UNIVERSITY OF AUCKLAND (Dr. Alick Kibblewhite, Dr. Gary Bold) | 2 |
| R.A.N. RESEARCH LAB. (Dr. Douglas Cato) | 1 |
| ADMIRALTY RES. EST. (Dr. David Weston) | 1 |